Tunneling Spectroscopy of an Electron Waveguide

Cristopher C. Eugster and Jesús A. del Alamo
Massachusetts Institute of Technology, Cambridge, Massachusetts 02139
(Received 6 September 1991)

On an AlGaAs/GaAs heterostructure, we have implemented a unique "leaky" electron waveguide with a thin tunneling barrier as one of its confining boundaries. The current flowing through the waveguide as well as the 1D to 2D tunneling current leaking out the thin side barrier were independently measured as the electron density in the waveguide was modulated. The tunneling current shows very strong oscillations lined up with the $2e^2/h$ conductance steps for the waveguide current. A proposed explanation is that the oscillations are a result of the 1D density of states sweeping through the Fermi level.

PACS numbers: 72.20.Jv, 73.40.Cg, 73.40.Gk, 73.40.Lq

The recent demonstration of electron waveguiding in high-mobility semiconductor heterostructures has not only uncovered a novel regime of electron transport in solids [1], but will perhaps lead to novel enhanced-functionality electronic devices [2]. In an electron waveguide, in close parallelism to electromagnetic waves in microwave and optical waveguides, electron propagation is determined by the discrete modes imposed by the confinement geometry. This strong analogy can be exploited in the search for novel devices and physics. Perhaps the most dramatic proof of electron waveguiding is the experimental observation of quantized conductance steps of magnitude $2e^2/h$ as the width of the waveguide is modulated [3–5].

In an effort to gain further insight into the physics of one-dimensional (1D) coherent electronic systems, we have carried out the first *tunneling spectroscopy of an electron waveguide.* This experiment has allowed us to directly observe the one-dimensional density of states of the waveguide. This has been realized through the implementation of a novel structure with a thin confining barrier which we refer to as a "leaky" electron waveguide.

The most versatile scheme for achieving narrow 1D channels in semiconductor heterostructures is the split-gate architecture [6]. A split-gate structure consists of a metal gate with a narrow slit on top of a modulation-doped heterostructure. A quantum wire is created by depleting the two-dimensional electron gas (2DEG) underneath the metal gates leaving a channel of a width comparable to the electron wavelength between the confining gates at the interface of the heterostructure. In this scheme the wire width and carrier density can be modulated through the fringing fields of the confining gates. Therefore, the relative position of the 1D subbands to the Fermi level can be controlled by means of the split-gate bias. If phase coherence is maintained through the wire and ionized impurity scattering is not present, then the 1D channel can be considered to be an electron waveguide [1,5].

In this work, we have taken the split-gate scheme one step further by implementing a leaky electron waveguide in which one of the split gates is very narrow, resulting in a thin confining potential sidewall. This allows us to not only monitor the current flowing through the waveguide but to simultaneously measure the leakage current flowing out the side of the waveguide. This tunneling current is expected to provide unique insight into the basic properties of 1D electron systems. In this Letter we report the observation of strong oscillations in the tunneling current flowing from the side of a wire that we interpret as direct spectroscopy of the 1D density of states of the electron waveguide.

Our devices [Fig. 1(a)] are designed with the ultimate goal of implementing a quantum-field-effect directional coupler [7]. Three metal gates are shaped to allow the formation of two electron waveguides that come in close proximity to each other over a certain length in what we term an intrinsic region. The two side gates can control the electron density in each waveguide independently. The thin middle gate controls the height and width of the potential barrier separating the two waveguides. For the results reported in this Letter we bias one of the side confining gates (herein referred to as the "bottom" gate) at 0 V so that the 2DEG underneath that gate is unaffected [Fig. 1(b)]. In this bias configuration, there is only one waveguide (formed by the "top" and "middle" gates) separated from a large 2DEG bath by a thin tunneling wall that can be controlled from the middle gate. Both the current flowing through the waveguide and the tunneling current out of the waveguide can be independently and simultaneously measured.

Fabrication of the devices began with molecular-beam-epitaxy growth of an AlGaAs/GaAs modulation-doped field-effect-transistor structure. The mobility of the 2DEG is 170000 $cm^2/V\,sec$ and the carrier density is 7×10^{11} cm^{-2} at 4 K. The 2DEG is at a depth of 545 Å from the semiconductor surface. Four alloyed Au/Ge/Ni Ohmic contacts, one at each corner, allow access to the two ends of each waveguide. The split-gate structure was defined using electron-beam lithography at the National Nanofabrication Facility (NNF) at Cornell University [8]. In order to minimize electron-beam writing time only the periphery of the top and bottom confining gates

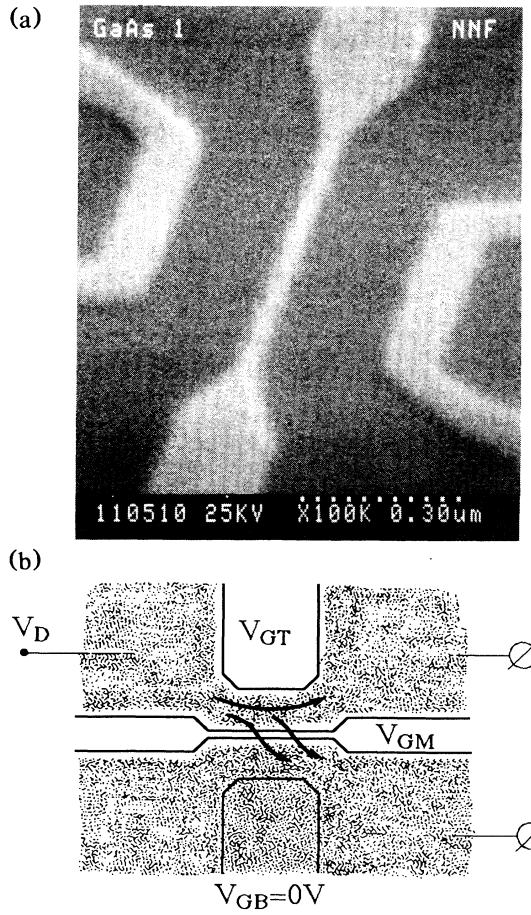

FIG. 1. (a) Scanning electron micrograph (SEM) of a split-gate structure used to implement a leaky electron waveguide. The middle gate, which serves as the tunneling barrier for the channel, is 30 nm wide. (b) Schematic of the biasing scheme for the implementation of the leaky electron waveguide. The shaded regions represent the electron concentration at the heterointerface.

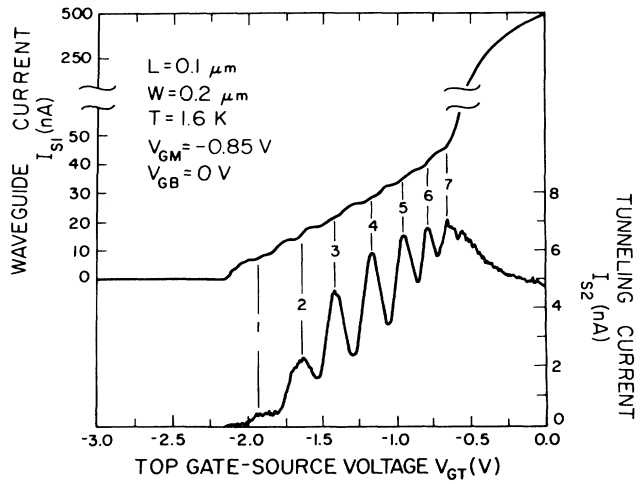

FIG. 2. The I_S-V_{GT} characteristics of the leaky waveguide. I_{S1} is the current flowing through the waveguide and I_{S2} is the tunneling current leaking out the thin side barrier. The tail region of I_{S1} has been expanded.

was drawn [9]. We fabricated several devices with the separation W between the side gates and the middle gate being 0.2 or 0.25 μm and the length L of the intrinsic portion of the split gates ranging from 0.1 to 0.5 μm. The middle gate in the intrinsic region was 30 nm wide and was fabricated using a single-pass e-beam lithography technique [8]. The middle gate was widened to 0.5 μm in the extrinsic region to provide isolation through short-channel effects.

The proper biasing configuration for the implementation of a leaky electron waveguide is shown in Fig. 1(b). The bottom-gate bias V_{GB}, as noted earlier, was set to 0 V in order to maintain a 2DEG underneath that gate. The middle-gate bias V_{GM} was chosen to provide perfect isolation in the extrinsic parts of the device, under the wider portions of the middle gate, yet still allow tunneling to take place in the intrinsic region. For our heterostructure, V_{GM} was -0.85 V. The bias on the top confining gate, V_{GT}, was swept negative from 0 V and was used to modulate the electron density in the waveguide.

An ac voltage, typically 100 μV, was applied across the waveguide with respect to ground. The contact to the side 2DEG was also grounded. Both grounds were actually the virtual grounds of two lock-in amplifiers working in the current mode that monitored the current flowing through the waveguide, I_{S1}, and the tunneling current, I_{S2}. The measurements were carried out at 1.6 K using standard lock-in techniques with $f=11$ Hz.

Under such a biasing scheme and for a $L=0.1$ μm, $W=0.2$ μm device, the waveguide current I_{S1} and the tunneling current I_{S2} were measured independently at 1.6 K as the top-gate bias V_{GT} was swept, as shown in Fig. 2. The waveguide current I_{S1} decreases as V_{GT} is made more negative, until at around $V_{GT}=-0.6$ V the 2DEG under the top gate is turned off and a 1D waveguide is formed. The ensuing long tail arises from the slow depletion of the electron concentration in the waveguide through the fringing field of the top gate. The waveguide turns off completely at $V_{GT}=-2.2$ V. The tunneling current I_{S2} through the thin middle barrier, measured simultaneously with I_{S1}, is also plotted in Fig. 2. Before the formation of the 1D waveguide the tunneling current is featureless. At the onset of formation of the top waveguide ($V_{GT}=-0.6$ V), strong oscillations are observed in the tunneling current I_{S2} as the carrier density in the channel is modulated. When the waveguide is turned off, the oscillations also disappear.

When we examine in detail the features in the tail region of the upper current I_{S1} shown in Fig. 2, we observe nearly quantized steps in the current. The rise of each step in I_{S1} roughly lines up with the onset of a new oscil-

lation in I_{S2}. There are approximately seven steps of conductance magnitude $2e^2/h$ for I_{S1} consistent with the total number of oscillations observed in I_{S2}. The deviation from perfect conductance quantization for I_{S1} is perhaps due to remote impurities [10] which might be expected in our relatively low-mobility sample. This is commonly observed for the higher-lying conductance steps of constrictions [5]. The oscillations in I_{S2} are reproducible and we have observed them in several different devices. They also are robust to temperature cycling all the way up to room temperature. The total number of oscillations is always consistent with the total number of steps in the tail region of the I_{S1}-V_{GT} characteristics for the different devices. For the wider devices ($W=0.25$ μm) eight oscillations were observed, resulting from the larger number of initial subbands occupied. The oscillations were also observed in the longer devices $L=0.5$ μm, while the conductance steps were much less visible at these lengths.

The oscillations washed out with increasing driving potential V_{DS} and with increasing temperatures. The oscillations are no longer visible for V_{DS} between 2 and 3 mV, as shown in Fig. 3. Temperature-dependent measurements showed that the oscillations disappear around 10 K.

We also studied the effect of changing the bias on the middle gate, V_{GM}, as shown in Fig. 4. There is an exponential suppression of the tunneling current when the barrier-gate voltage is made more negative. However, the peaks and valleys of the oscillations line up. The steps in I_{S1} also do not shift significantly with small changes in the middle-gate voltage since small changes in V_{GM} strongly affect I_{S2} without significantly modifying the carrier density in the waveguide.

All our experimental observations are consistent with a picture in which the oscillations in the tunneling current constitute electron spectroscopy of the waveguide. The quantized conductance steps of magnitude $2e^2/h$ observed for the waveguide current suggest that near ballistic transport is taking place in it. The onset of each step corresponds to the sweeping of a 1D density of states (DOS) subband through the Fermi level [3,4]. The current flowing through the waveguide is proportional to the product of the 1D DOS, g^{1D}, and the electron wave vector in the direction of the current flow, $k_{\|}$. The 1D DOS is inversely proportional to the square root of the energy of the electrons while $k_{\|}$ is proportional to it, thereby resulting in a constant product. This gives rise to the constant steps in the current observed in the tail region of I_{S1}.

An expression for the tunneling current I_{S2} tunneling through the sidewall of the waveguide can be arrived at by the following integral:

$$I_{S2}=e\sum_j \int_{-\infty}^{\infty} v_{\perp j}(E-E_j)g_j^{1D}(E-E_j)T_j(E-E_b) \times[f(E-E_F-e\Delta V,T)-f(E-E_F,T)]\,dE\,, \tag{1}$$

where we have accounted for the contribution to the current from each occupied subband j. E_j is the energy at the bottom of the jth subband and E_b is the height of the tunneling energy barrier. The normal velocity against the tunneling barrier is $v_{\perp j}(E)=\hbar k_{\perp j}/m^*$. The transmission coefficient, $T_j(E-E_b)$, to first order, is the same

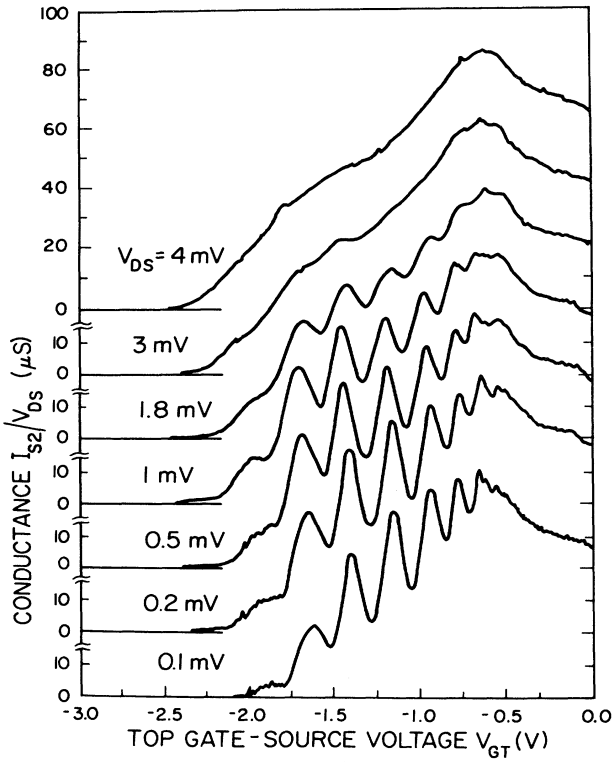

FIG. 3. Tunneling conductance I_{S2}/V_{DS} for increasing values of V_{DS}. The oscillations wash out between 2 and 3 mV. The gate biases are the same as in Fig. 1(b).

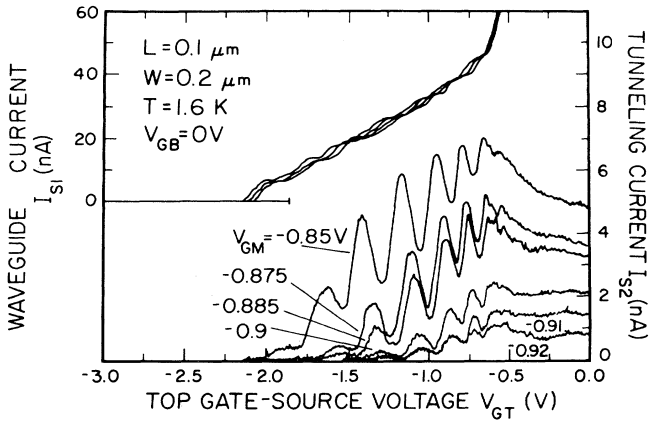

FIG. 4. The I_S-V_{GT} characteristics for increasing values of the middle-gate bias V_{GM}.

for the different subbands since the barrier height relative to the Fermi level E_F is fixed. The Fermi function f gives the distribution of the electrons as a function of temperature and applied bias ΔV across the input of the waveguide and the 2DEG on the other side of the tunneling barrier. ΔV determines the window of injected electron energies and differs from V_{DS} by the potential drops across the series and contact resistances. At low temperatures these resistances are negligible ($\approx 200\ \Omega$).

For low enough temperatures and a narrow window of injected electrons around the Fermi level, we can approximate Eq. (1) as

$$I_{S2} \cong \frac{e^2\hbar}{m^*} \sum_j k_{\perp j} T_j(E_F - E_b) g_j^{1D}(E_F - E_j) \Delta V , \qquad (2)$$

where $k_{\perp j}$ is a constant for each subband due to lateral quantization and has a value determined by the confining potential. As seen by Eq. (2), the tunneling current I_{S2} is proportional to $g^{1D}(E_F - E_j)$. Modulating V_{GT} sweeps the subbands through the Fermi level and since $k_{\perp j}$ and $T_j(E_F - E_b)$ are constant for a given subband, I_{S2} reproduces the 1D density of states g^{1D} for each subband. It is important to note that in sweeping V_{GT}, the Fermi level is unaffected with respect to the top of the tunneling barrier E_b since V_{GM} is fixed at a constant value.

The effects of finite temperature and voltage present in the experiment result in a washing out of the features of I_{S2} from the g^{1D} [Eq. (1)]. Finite voltage averages the current over an energy range $e\Delta V$ near E_F while finite temperature averages the current over a region $3.5kT$ around E_F [11]. When the energy of this window of injected electrons into the waveguide, determined by the bias and temperature, approaches the intersubband spacing, the resolution of tunneling from a single subband diminishes. In our results both the finite voltage and temperature broadening indicate a characteristic energy of 2–3 meV at which the oscillations wash out. This characteristic energy is in good agreement with the subband spacings which have been calculated for similar split-gate wires [12].

In trying to understand why the oscillations persist in the longer devices ($L = 0.5\ \mu$m) while the quantized plateaus in I_{S1} are much less visible, we must address the issue of where the tunneling occurs in the waveguide. Since the tunneling barrier is thinnest at the center of the intrinsic region, tunneling is likely to occur mainly under a small region (towards the center) of the middle gate. If there is no mode mixing in this region, then we expect the oscillations to be clearly observable, even if the plateaus are not.

In summary, we have fabricated a 1D electron waveguide in which the tunneling current out of a leaky sidewall shows strong oscillations as the electron density in the waveguide is modulated. Our experimental observations are consistent with a picture in which the tunneling current is directly mapping out the 1D DOS of the waveguide. Our experiment constitutes a novel tunneling spectroscopy that provides insight into the fundamental physics of 1D electron systems.

We would like to acknowledge M. J. Rooks for electron-beam lithography at NNF, Cornell University, C. G. Fonstad and K. Ismail for epitaxial sample growth, and M. A. Kastner, H. I. Smith, P. Lee, Q. Hu, and T. P. Orlando for stimulating discussions. This work has been funded by NSF Contracts No. 87-19217-DMR and No. DMR-9022933. C.C.E. acknowledges an IBM Graduate Fellowship award.

[1] C. W. J. Beenakker and H. van Houten, in *Solid State Physics, Semiconductor Heterostructures and Nanostructures,* edited by H. Ehrenreich and D. Turnbull, (Academic, New York, 1991), p. 1.

[2] A. J. Holden, in *Gallium Arsenide and Related Compounds 1990,* edited by K. Singer, IOP Conf. Proc. No. 112 (Institute of Physics and Physical Society, London, 1991), p. 1.

[3] B. J. van Wees, H. van Houten, C. W. J. Beenakker, J. G. Williamson, L. P. Kouwenhoven, D. van der Marel, and C. T. Foxon, Phys. Rev. Lett. **60**, 848 (1988).

[4] D. A. Wharam, T. J. Thornton, R. Newbury, M. Pepper, H. Ahmed, J. E. F. Frost, D. G. Hasko, D. C. Peacock, D. A. Ritchie, and G. A. C. Jones, J. Phys. C **21**, L209 (1988).

[5] G. Timp, R. Behringer, S. Sampere, J. E. Cunningham, and R. E. Howard, in *Nanostructure Physics and Fabrication,* edited by M. A. Reed and W. P. Kirk (Academic, New York, 1989), p. 331.

[6] T. J. Thornton, M. Pepper, H. Ahmed, D. Andrews, and G. J. Davies, Phys. Rev. Lett. **56**, 1198 (1986).

[7] J. A. del Alamo and C. C. Eugster, Appl. Phys. Lett. **56**, 78 (1990).

[8] M. J. Rooks, C. C. Eugster, J. A. del Alamo, G. L. Snider, and E. L. Hu, J. Vac. Sci. Technol. B (to be published).

[9] C. C. Eugster, J. A. del Alamo, and M. J. Rooks, Jpn. J. Appl. Phys. **29**, L2257 (1990).

[10] J. A. Nixon, J. H. Davies, and H. U. Baranger, Phys. Rev. B **43**, 12638 (1991).

[11] P. F. Bagwell and T. P. Orlando, Phys. Rev. B **40**, 1456 (1989).

[12] G. L. Snider, I.-H. Tan, and E. L. Hu, J. Appl. Phys. **68**, 5922 (1990).

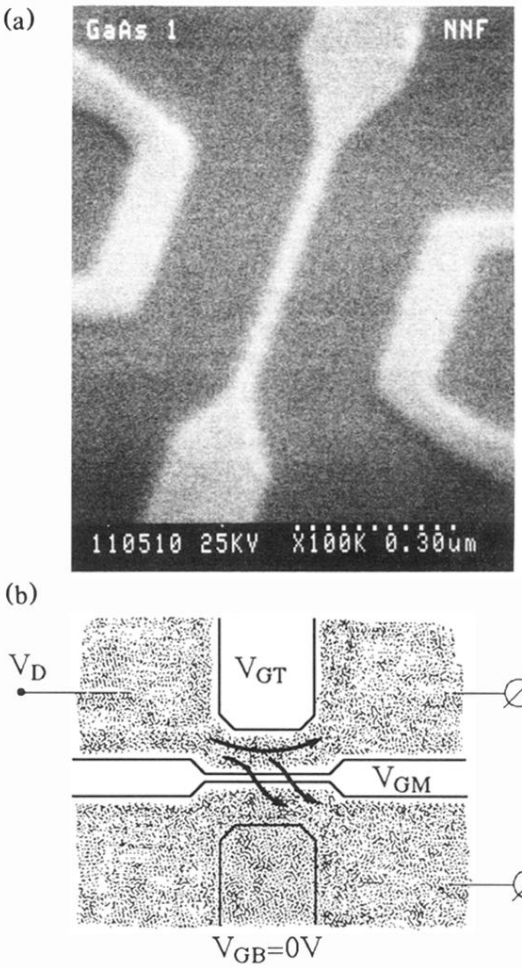

FIG. 1. (a) Scanning electron micrograph (SEM) of a split-gate structure used to implement a leaky electron waveguide. The middle gate, which serves as the tunneling barrier for the channel, is 30 nm wide. (b) Schematic of the biasing scheme for the implementation of the leaky electron waveguide. The shaded regions represent the electron concentration at the heterointerface.